

SOLUTION MINING RESEARCH INSTITUTE

679 Plank Road
Clifton Park, NY 12065, USA

Telephone: +1 518-579-6587
www.solutionmining.org

**Technical
Conference
Paper**



Effect of the Addition of a Low Equivalent Stress Creep Mechanism to the Analysis of Geomechanical Behavior of the SPR West Hackberry Site

Steven R. Sobolik and Tonya S.A. Ross
Sandia National Laboratories, Albuquerque, NM, USA

**SMRI Fall 2021 Technical Conference
20-21 September 2021
Galveston, Texas, USA**

Effect of the Addition of a Low Equivalent Stress Creep Mechanism to the Analysis of Geomechanical Behavior of the SPR West Hackberry Site

Steven R. Sobolik and Tonya S.A. Ross

Sandia National Laboratories, Albuquerque, New Mexico, USA

Abstract

Sandia National Laboratories has long used the Munson-Dawson (M-D) model to predict the geomechanical behavior of salt caverns used to store oil at the Strategic Petroleum Reserve (SPR). Salt creep causes storage caverns to deform inward, thus losing volume. This loss of volume affects the salt above and around the caverns, puts stresses and strains on borehole casings, and creates surface subsidence which affects surface infrastructure. Therefore, accurate evaluation of salt creep behavior drives decisions about cavern operations. Parameters for the M-D model are typically fit against laboratory creep tests, but nearly all historic creep tests have been performed at equivalent stresses of 8 MPa or higher. Creep rates at lower equivalent stresses are very slow, such that tests take months or years to run, and the tests are sensitive to small temperature perturbations ($<0.1^{\circ}\text{C}$). A recent collaboration between US and German researchers, however, recently characterized the creep behavior at low equivalent (deviatoric) stresses (<8 MPa) of salt from the Waste Isolation Pilot Plant. The M-D model was recently extended to include a low stress creep “mechanism”. This paper details new simulations of SPR caverns at the West Hackberry site that use this extended M-D model, called the M-D Viscoplastic model. The results show that the inclusion of low stress creep significantly alters the prediction of steady-state cavern closure behavior and indicate that low stress creep is the dominant displacement mechanism at the dome scale. This paper also describes the changes to predicted stresses and strains that impact cavern and wellbore integrity. The results of the calculations in this paper indicate the need for laboratory creep tests at low equivalent stresses on salt from storage cavern sites. This knowledge will help to improve evaluation of storage cavern behavior in salt domes.

Key words: Caverns for Gas Storage, Caverns for Liquid Storage, Creep, Computer Modeling, Instrumentation and Monitoring, Rock Mechanics

Introduction

The U.S. Strategic Petroleum Reserve (SPR), operated by the U.S. Department of Energy (DOE), stores crude oil in solution-mined caverns in the salt dome formations of the Gulf Coast. There is a total of 60 storage caverns located at four different sites in Texas (Bryan Mound and Big Hill) and Louisiana (Bayou Choctaw and West Hackberry), along with several abandoned or decommissioned caverns. Each cavern is constructed and then operated using a wellbore or wellbores that are lined with steel casings cemented in place from the surface to near the top of the cavern. The West Hackberry salt dome is in the extreme southwestern corner of Louisiana, some 24 km from the Louisiana/ Texas border to the west and the Gulf of Mexico to the south. It has an oil storage capacity of about $35 \times 10^6 \text{ m}^3$ (222×10^6 barrels) within 21 caverns, and has operated since 1980.

Sandia National Laboratories (SNL) has served as a technical advisor on the SPR to DOE since 1980. As part of that responsibility, SNL has long used computational geomechanical models to analyze the viscoplastic, or creep, behavior of the salt in which the oil storage caverns reside. Salt creep causes storage caverns to deform inward, thus losing volume. This loss of volume affects the salt above and around the caverns, puts stresses and strains on borehole casings, and creates surface subsidence which affects

surface infrastructure. Therefore, accurate evaluation of salt creep behavior drives decisions about cavern operations.

To perform geomechanical computational analyses of the SPR sites, SNL has used the Sierra/Solid Mechanics (2018) finite element code. Sierra/SM has many different constitutive models for viscoplastic behavior, including the Munson-Dawson (M-D) constitutive model for salt. The M-D model was originally developed in the 1980s to predict the thermomechanical behavior of rock salt [Munson & Dawson, 1979 & 1982; Munson et al., 1989]. Since then, it has been used to simulate the evolution of the underground in nuclear waste repositories, mines, and storage caverns for gases and liquids. A recent collaboration between US and German researchers interested in the utilization of salt formations for nuclear waste repositories has recently benchmarked salt creep models against room closure measurements. The Waste Isolation Pilot Plant (WIPP) in southeastern New Mexico consists of excavated rooms within a bedded salt formation for the permanent storage of transuranic waste. Simulations of Room D at WIPP using the M-D model under-predicted the room's vertical closure rate by a factor of 2.8 at 3.7 years after room excavation [Reedlunn, 2016, 2018a]. The M-D model numerical implementations in Sierra/SM also ran quite slowly during these simulations. As a result, three enhancements were made to the M-D model in [Reedlunn, 2018b]. (1) The calculation of equivalent stress was changed to a more generalized formulation proposed by Hosford [1972]. (2) New transient and steady-state rate terms were added to capture salt's creep behavior at low equivalent stresses (below about 8 MPa). (3) The M-D model's numerical implementation was overhauled, adding a line search algorithm to the implicit solution scheme. The first enhancement was described in detail in Reedlunn [2018b] and Sobolik and Ross [2021], but it is the second enhancement, the addition of a low equivalent stress creep component to the M-D model, that is the primary subject of this paper. This newly enhanced M-D model is being called the M-D Viscoplastic model [Sobolik & Ross, 2021]. The results presented in this paper will show that the inclusion of low equivalent stress creep significantly improves the prediction of steady-state cavern closure behavior. In addition, predictions of vertical strain in the borehole casings are significantly different using the new model.

M-D Viscoplastic Model Description

Plastic deformation of intact salt only occurs in the presence of shear stress. Shear stress only occurs when the three principal normal stresses are unequal; such an anisotropic stress state is also called deviatoric stress. Originally, the M-D model utilized the von Mises stress as its equivalent shear stress measure σ_{eq} , but Munson et al. [1989] switched σ_{eq} to the Tresca stress. Both of these formulations are specific instances of a more general formulation for an equivalent stress measure proposed by Hosford [1972]. The Hosford stress is given by

$$\sigma_{eq} = \left\{ \frac{1}{2} (|\sigma_1 - \sigma_2|^a + |\sigma_2 - \sigma_3|^a + |\sigma_3 - \sigma_1|^a) \right\}^{1/a}, \quad (1)$$

where σ_i are the principal stresses and a is a material parameter. For the Tresca equivalent stress, a can be 1 or ∞ (these derive the same values – see Reedlunn [2018b] for derivation), and for von Mises stress, a can be 2 or 4 (also equivalent, see Reedlunn [2018b]). For the calculations using the M-D Viscoplastic model presented in this paper, the equivalent stress was calculated using a value for a of 100 [Sobolik & Ross, 2021].

The original M-D creep model additively decomposed the steady state creep behavior of salt into three “mechanisms” [Munson, 1998]. Mechanism 1 is meant to capture dislocation climb, which dominates at high temperatures and low equivalent stresses. Mechanism 2 dominates at low temperatures and medium equivalent stresses, and is the dominant mechanism measured in laboratory creep tests of SPR salts and salts from the Waste Isolation Pilot Plant (WIPP) in southeastern New Mexico. Mechanism 3 is negligible for the stress states experienced at SPR sites and will not be discussed here. A more complete description of the entire model is given in Park [2020]; the equations for Mechanisms 1 and 2 (and which was chosen for Mechanism 0 as explained later) are:

$$\dot{\epsilon}^{ss} = \sum_{i=0}^3 \dot{\epsilon}_i^{ss} \quad (2)$$

$$\dot{\epsilon}_i^{ss} = A_i \exp\left(-\frac{Q_i}{RT}\right) \left(\frac{\sigma_{eq}}{\mu}\right)^{n_i} \text{ for } i = 0, 1, \text{ and } 2, \quad (3)$$

where A_i is the creep constant for each mechanism, n_i is the creep exponent, Q_i is the activation energy, R is the universal gas constant, and T is the absolute temperature of the salt. The original M-D model input parameter values for West Hackberry are based on laboratory creep tests using core samples from two boreholes [Munson, 1998]; these parameters are shown in Table 1. In addition, for previous SPR geomechanical analyses multiplication factors were applied to the steady-state creep coefficient A_2 for Mechanism 2 in Equation 3, and the transient creep coefficient K_0 . These multiplication factors were used to try to match predictions of surface subsidence and cavern volume closure to historical subsidence data and calculated cavern volume closure from wellhead pressure data using the software CAVEMAN [Ballard and Ehgartner, 2000]. For both Bryan Mound and West Hackberry calculations, it was much easier to match the surface subsidence data than the cavern volume closure histories [Sobolik 2015, 2018]. In particular, it has been difficult to predict match the steady-state cavern closure rate using the M-D model in its original formulation.

Table 1. M-D model mechanical parameters published for West Hackberry salt [Munson, 1998].

Property or parameter	Values
Density, lb/ft ³	144 (2300 kg/m ³)
Elastic modulus, lb/ft ²	648 × 10 ⁶ (31.0 GPa)
Shear modulus, lb/ft ²	259 × 10 ⁶ (12.4 GPa)
Poisson's ratio	0.25
Primary Creep Constant A_1 , sec ⁻¹	9.81 × 10 ²²
Exponent n_1	5.5
Q_1 , cal/mol	25000
Secondary Creep Constant A_2 , sec ⁻¹	1.13 × 10 ¹³
Exponent n_2	5.0
Q_2 , cal/mol	10000
B_1 , sec ⁻¹	7.121 × 10 ⁶
B_2 , sec ⁻¹	3.55 × 10 ⁻²
σ_0 , lb/ft ²	429 × 10 ³ (20.57 MPa)
q	5335
m	3.0
K_0 (changed to K_1 in M-D viscoplastic model)	6.275 × 10 ⁵
c (1/R) (0.009198/1.8)	0.00511
A	-17.37
B	-7.738
Δ	0.58

The M-D model relies on laboratory creep test data to obtain parameters to model steady-state creep behavior. However, nearly all laboratory creep testing has been performed at equivalent stresses of 8 MPa or higher. The primary reason that tests have not been performed at lower equivalent stresses is that the creep rates are very slow so the tests take months or years to run, and they are very sensitive to small temperature perturbations (<0.1°C). Despite these difficulties, several researchers (e.g. Bérest et al. [2005], Bérest et al. [2019], Salzer et al. [2015], and Düsterloh et al. [2015]), have reported larger steady-state creep rates at than would be expected from extrapolating rates from higher stresses.

To capture the low equivalent stress behavior, Reedlunn [2018b] added a fourth mechanism to the M-D model. The micro-mechanical mechanism responsible for the creep behavior at low equivalent stresses is

probably pressure solution redeposition [Peach et al. 2001; Ter Heege et al. 2005a; Ter Heege et al. 2005b; J. Urai et al. 2008; Bérest et al. 2019], but Mechanism 0 was given the same mathematical form as Mechanisms 1 and 2 for simplicity. For the extended M-D Viscoplastic model, the addition of the low equivalent stress mechanism (Mechanism 0) is expected to accommodate the creep experienced by the large volume of salt between the caverns existing at that low stress state. Reedlunn [2018] calibrated the parameter values for Mechanism 0 in Eq. (3) against the Salzer et al. [2015], and Düsterloh et al. [2015] experiments on WIPP salt. His values for the Mechanism 0 parameters in Equation 3 are listed in Table 2. Reedlunn used a value of 16 for the Hosford exponent in Eq. 1; for the calculations performed for this paper a value of 100 was used as it improved computational speed. Due to a lack of currently available test data on SPR salt, these parameters will be used in the extended M-D Viscoplastic model for the SPR.

Table 2. M-D Viscoplastic model low stress steady-state strain rate parameters [Reedlunn, 2018].

Parameter	Value
Low Equivalent Stress Creep Constant A_0 , sec^{-1}	56.17
Exponent n_0	1.595
Q_0 , cal/mol	10000

Figure 1 shows how the implementation of the low equivalent stress mechanism would change the steady-state strain rate as a function of stress. Strain rate is plotted as a function of equivalent stress for both the original M-D and extended M-D Viscoplastic models, using the original Munson properties for Bryan Mound and West Hackberry salt and the Table 2 properties for Mechanism 0. Also show in Figure 1 are the typical range of stresses at which laboratory creep tests are performed (8-20 MPa), which usually occur within a few feet of the cavern walls, and the lower stress range (1-8 MPa), which occurs in most of the inter-cavern or pillar salt. Even though the strain rates predicted by mechanism 0 are 2-3 orders of magnitude less than strain rates in the normal testing range, those small strain rates over a much larger volume of salt could have profound effects on the overall behavior of the dome.

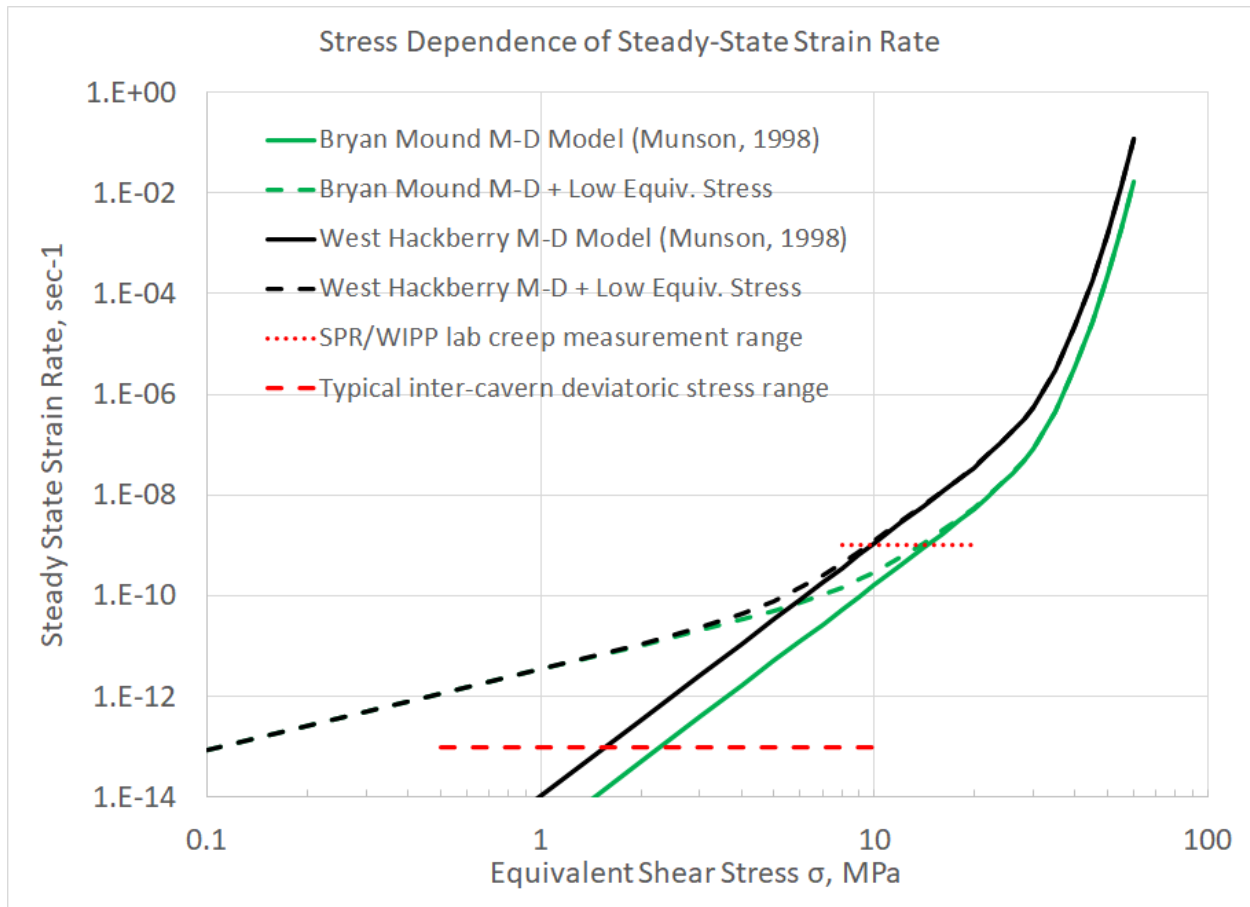


Figure 1. Effect of additional low equivalent stress mechanism in M-D viscoplastic model.

Computational Model for the West Hackberry Site

This section describes the geomechanical model of the SPR West Hackberry salt dome. The West Hackberry site consists of 22 caverns. Figure 2 shows the relative locations and geometries of these caverns. The SPR purchased five existing caverns in the early 1980s. These five Phase 1 caverns – Caverns 6, 7, 8, 9, and 11 – were created as early as 1946 and were used for brine production and storage before the SPR took ownership of them. After that time, seventeen other storage caverns (numbered 101 to 117) were created over an eight-year period. The post-1981 caverns were built via solution mining, and all have a generally cylindrical shape (more specifically, frustums with the larger diameter at the top) of approximately 600 m (2000 feet) height and 30-45 m (100-150 feet) in radius. The Phase 1 caverns, however, were originally built for brine production, and thus they were constructed with less concern about the long-term stability of the cavern shape. Cavern 6 at the West Hackberry site has an unusual dish-like shape with a large rim around the circumference. The diameter of Cavern 6 at the ceiling ranges from 340 to 380 meters. It is also in close proximity to Cavern 9, an hourglass-shaped cavern.

The mesh for the computational model is illustrated in Figures 3 and 4. Figure 3 shows the entire mesh used for these calculations, and Figure 4 shows the same view with the overburden and caprock removed to expose the salt formation (in magenta and yellow). The mesh comprises 5.99 million nodes and 5.95 million hexahedral elements. Four material blocks are used in the model to describe the stratigraphic layers: the overburden, caprock, salt dome and sandstone surrounding the salt dome. The overburden is made of unconsolidated sand, and the caprock layer is made of gypsum and limestone. These materials were modeled as elastic materials [Sobolik, 2015]. The overburden layer is 480 m thick, and the caprock is 120 m in the central portion of the dome. In an attempt to include the downward contour of the top of the salt dome at its outer perimeter, an outer ring of caprock has a total thickness of 240 m.

Figure 5 highlights the volume of one of the caverns, WH-101, in both its computational mesh geometry and its oldest available sonar geometries from 2000 and 2006, and the geometries of the five drawdown layers (i.e., layers of growth related to salt dissolution from oil drawdowns) built into the computational mesh. All of the caverns were meshed similarly.

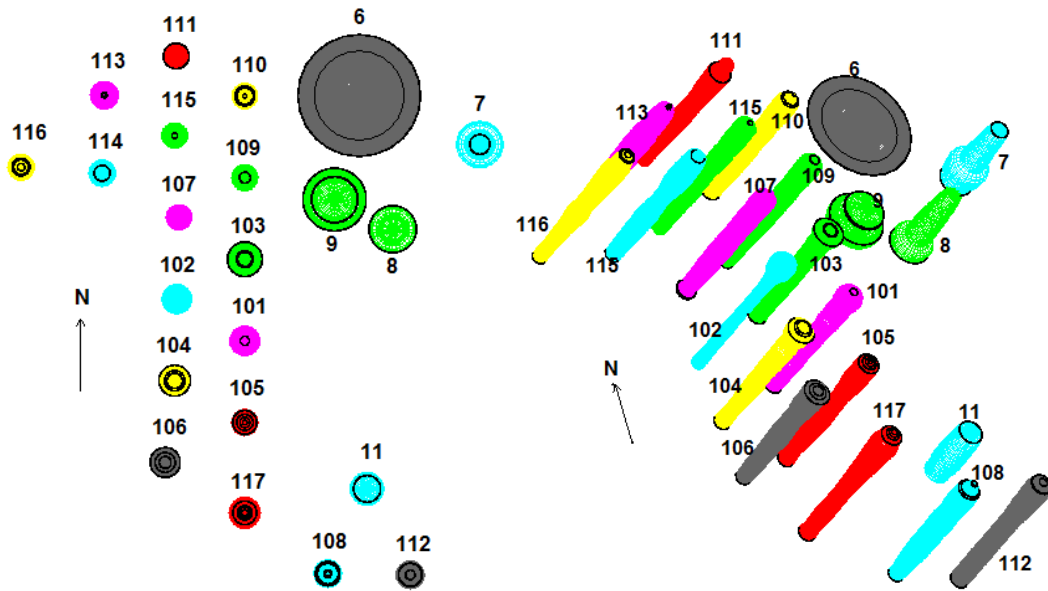


Figure 2. West Hackberry caverns included in the computational mesh (2 views).

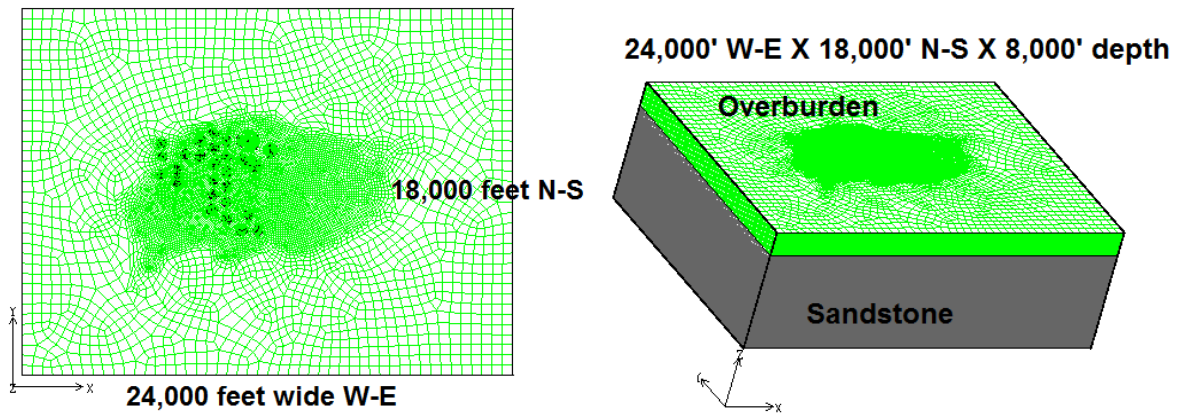


Figure 3. Computational mesh, full-dome West Hackberry model.

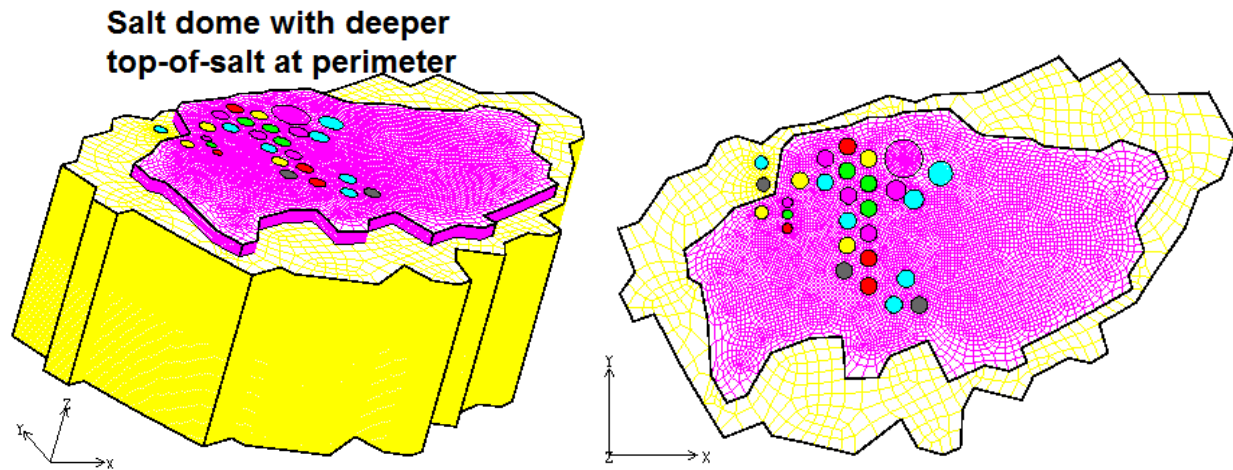


Figure 4. Computational mesh showing the salt dome and cavern locations.

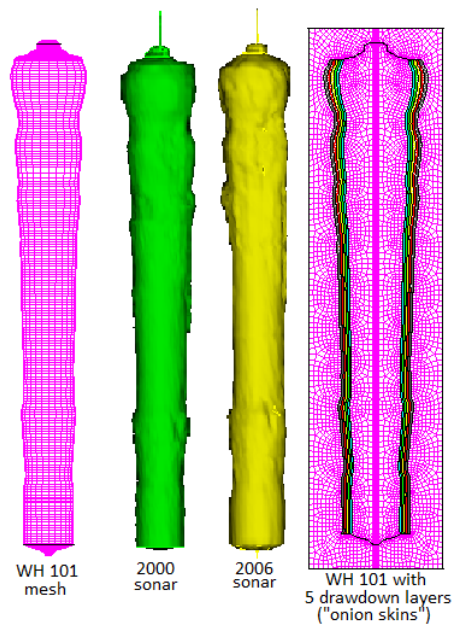


Figure 5. Computational mesh, sonar geometries for WH-101.

Predictions of subsidence and cavern closure

This section describes the results of several different sets of model calculations with the geomechanical model of the SPR West Hackberry salt dome for which the salt constitutive model parameters are varied. The results will compare predicted values for cavern volume closure and surface subsidence to values measured at the West Hackberry site.

The classic M-D material properties for West Hackberry salt were based on laboratory data from core samples [Munson, 1998]; these properties are listed in Table 1. In addition, for the 2015 WH model calculations [Sobolik, 2015] multiplication factors were applied to the steady-state creep coefficient A_2 for Mechanism 2 in Equation 3, and the transient creep coefficient K_0 . (This is the nomenclature used in the original M-D model – the same coefficient is called K_1 in the M-D Viscoplastic model.) These multiplication factors are listed in Table 3; these multiplication factors were applied to the cylinder of salt surrounding each respective cavern, as seen in Figures 4 and 5. Figure 6 shows the measured cavern volume closure along with predictions from the 2015 WH model calculations through 2015 [Sobolik, 2015] (results are for Phase 2 caverns on the east side of the site). For all the figures from this point forward, solid lines are used

for measurements, dashed lines for prediction results. Even with a variety of multiplication factors applied to A_2 and K_0 individually for regions around each cavern, it was difficult to match the steady-state closure rate. The large jumps in each closure history represent workovers, which are cavern maintenance periods during which the wellhead pressure is reduced to zero for a period of one to six months; in the computational model, the workovers are modeled as three month events, which is most typical. During workovers, the transient component is temporarily dominant. These large volume changes help to give a time-averaged prediction of cavern closure that roughly matches the measured values, but this type of match is not desirable. Figure 7 shows the measured surface subsidence at cavern well locations along with predictions from the 2015 WH model calculations. The predicted values match the measured values very well, which in part led to the decision to use the set of parameters applied to the 2015 model.

Table 3. Multiplication factors applied to the A_2 values listed in Table 1 for Sobolik [2015] analyses of West Hackberry.

Cavern	A_2 multiplication factor	Cavern	A_2 multiplication factor
101	1.44	112	1.21
102	2.44	113	1.77
103	2.08	114	1.43
104	1.79	115	1.51
105	2.79	116	3.20
106	1.48	117	1.73
107	2.24	6	1.44
108	1.73	7	1.67
109	1.46	8	0.89
110	2.35	9	1.96
111	2.42	11	1.21
WH Salt	1.80		
K_f , Multiplication factor for K_0 in transient creep equation (i.e., K_0 used in analysis = $(K_{0, Munson}) * (K_f)$			$K_f=18.2$

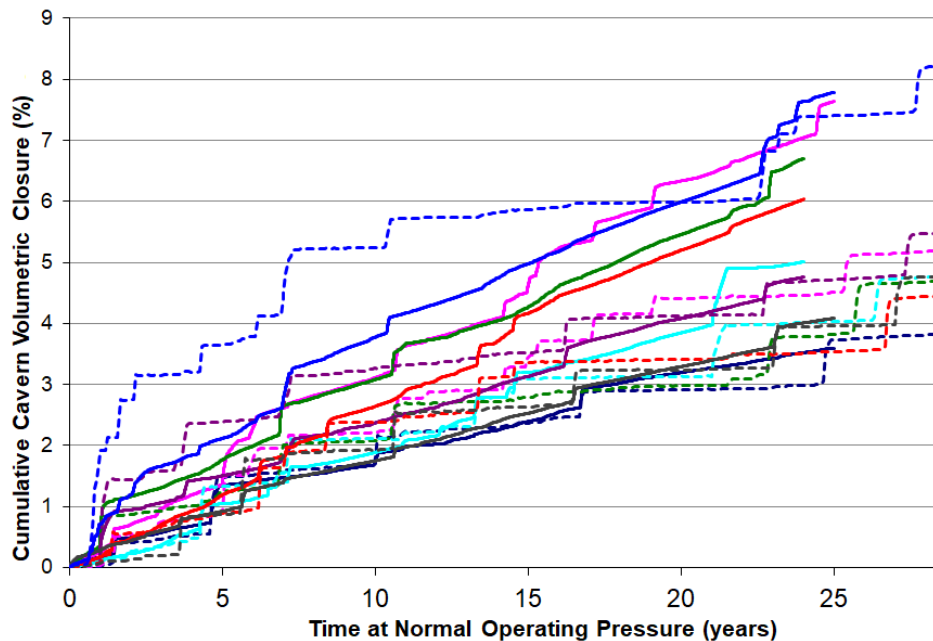
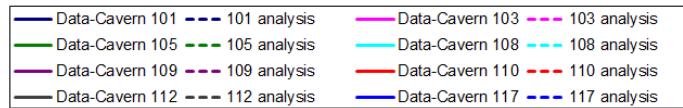


Figure 6. Comparison of West Hackberry predicted cavern closure vs. measurements, 2015 WH M-D properties [Sobolik, 2015].

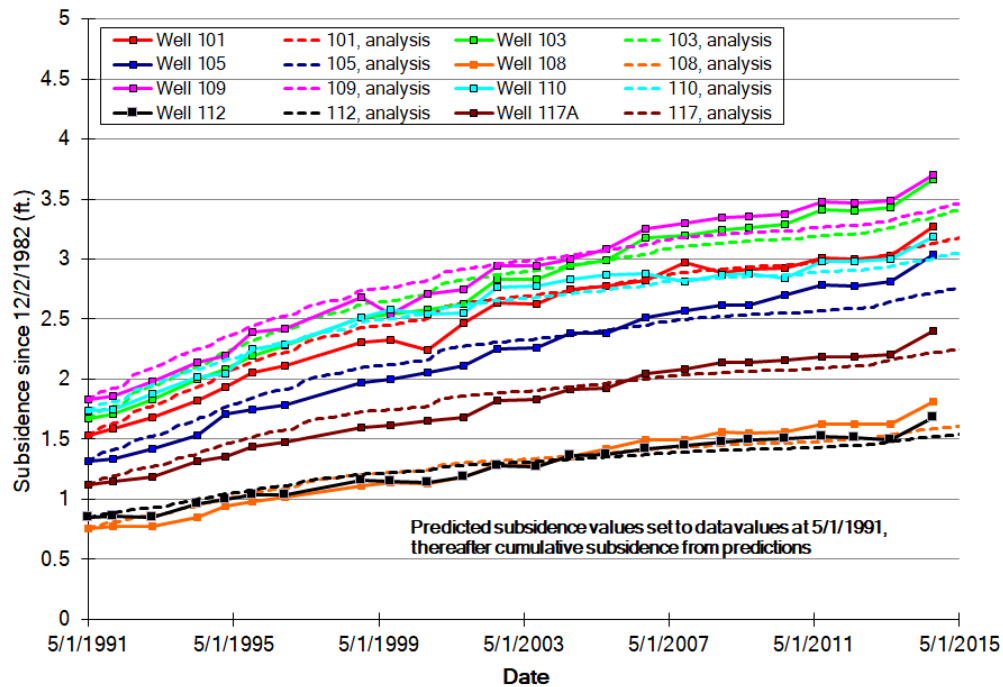


Figure 7. Comparison of West Hackberry predicted surface subsidence vs. measurements, 2015 WH M-D properties [Sobolik, 2015].

The use of Mechanism 0 in the M-D Viscoplastic model had a significant effect on predictions of cavern volume closure and surface subsidence at West Hackberry. Figure 8 shows the same measured cavern volume closure as Figure 6, but the predictions utilized Mechanism 0. For these calculations, the A2 and transient creep K0 (now renamed K1 in the new model) multiplication factors are the same as used for the 2015 analysis (Table 3), with the low equivalent stress Mechanism 0 included (Table 2), with the Hosford exponent $a=100$. It is obvious that the addition of the low stress creep over a large volume of salt has added greatly to the predicted cavern closure rates. The steady-state closure rates between workovers, as indicated by the slopes of the curves in Figure 8, are much more similar to the measured closure rates. Figure 9 shows the effects of adding the low stress creep mechanism on the predicted surface subsidence. The predicted values are significantly higher than the 2015 predictions and the measured data.

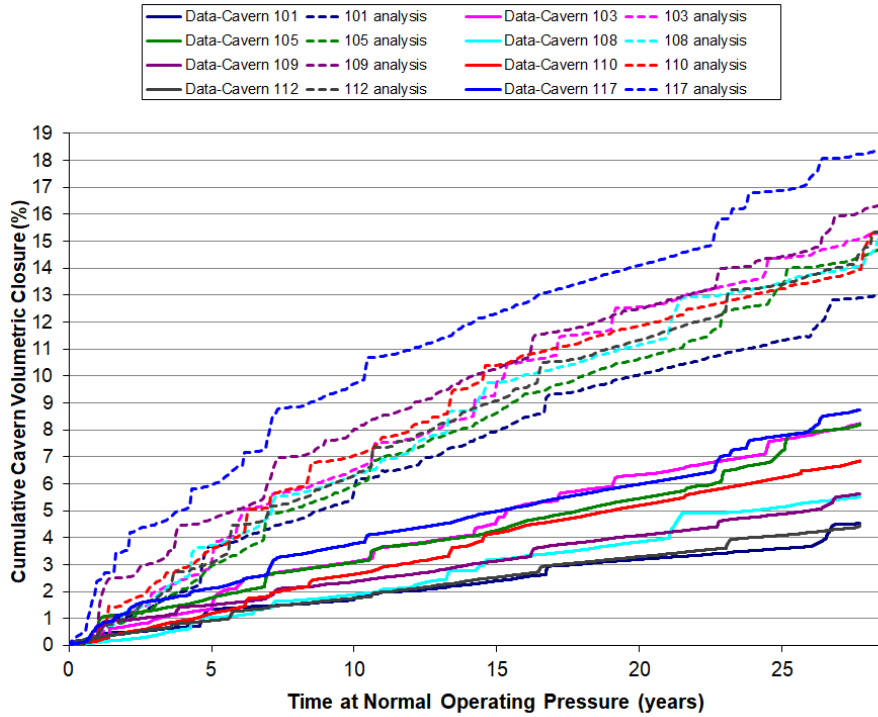


Figure 8. Comparison of West Hackberry predicted cavern closure vs. measurements, 2015 WH M-D properties plus low equivalent stress component (Mechanism 0).

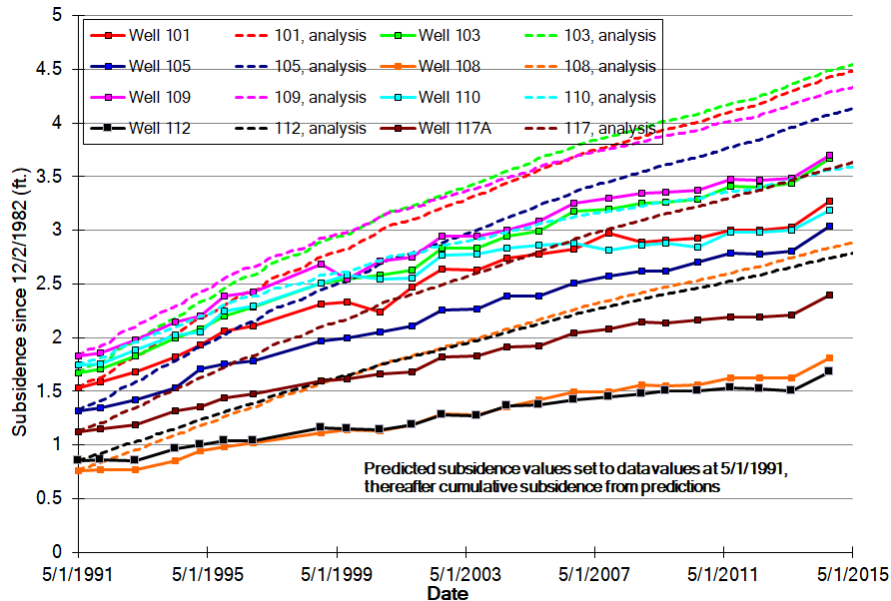


Figure 9. Comparison of West Hackberry predicted surface subsidence vs. measurements, 2015 WH M-D properties plus low equivalent stress component (Mechanism 0).

Because the steady-state creep of the salt has been greatly enhanced by the addition of Mechanism 0, it is now possible to perform new calculations with values of A_2 and K_1 closer to those captured experimentally in Munson [1998], which would better honor the fidelity of the previous laboratory data. A set of calculations was performed with the M-D Viscoplastic model for which all the multiplication factors in Table 2 were eliminated (that is, made equal to 1), thus using the original M-D creep parameters in Table 1 unmodified,

along with the Mechanism 0 creep using the parameters in Table 2. It was expected that there would be a noticeable decrease in predicted steady-state creep rates and overall cavern closure and subsidence from the results in Section 4.2. Figures 10 and 11 show the results for cavern volume closure and surface subsidence, respectively. Although the predicted values were indeed somewhat less when removing the previous multiplication factors, the magnitude of the difference is small when compared to the overall magnitudes. This small difference seems to indicate that on a domal scale, the low equivalent stress dominates the overall displacement of salt in the dome. This would potentially be due to the much larger volume of salt between and around the caverns that experiences the smaller stress states, than the volume of the thin skins around the cavern that experience the stress states historically imposed in laboratory creep tests.

Figures 12 and 13 show contour plots of the predicted equivalent stress in MPa for two vertical slices through the dome. Figure 12 shows a slice through the approximate center of the cavern field where Cavern 103 is located. The slice in Figure 13 runs through Caverns 107, 9, and 8. This slice is located through the point at which the highest value of equivalent stress is recorded during the calculations, a point on the bottom lobe of Cavern 9 which is close to Cavern 8 during a workover on that cavern. It is important to notice that his maximum value is nearly 15 MPa and is small enough in this view to be difficult to see, but only small regions in the immediate vicinity of the caverns experience equivalent stresses over 7.5 MPa. Much larger volumes of salt experience equivalent stresses between 1 and 7.5 MPa. It is the creep of these much larger volumes at lower stresses that has not previously been captured in laboratory creep tests. As the calculations presented in the paper indicate, the deformation of this larger volume may have a more significant effect on the overall deformation of the salt dome and caverns than the higher stressed regions in the walls surrounding each cavern.

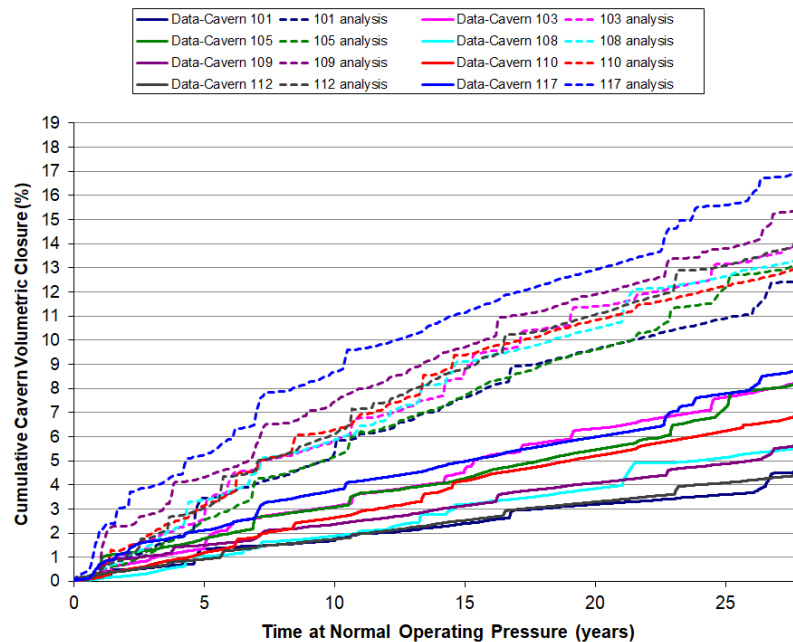


Figure 10. Comparison of West Hackberry predicted cavern closure vs. measurements, original WH M-D properties plus low equivalent stress component (Mechanism 0).

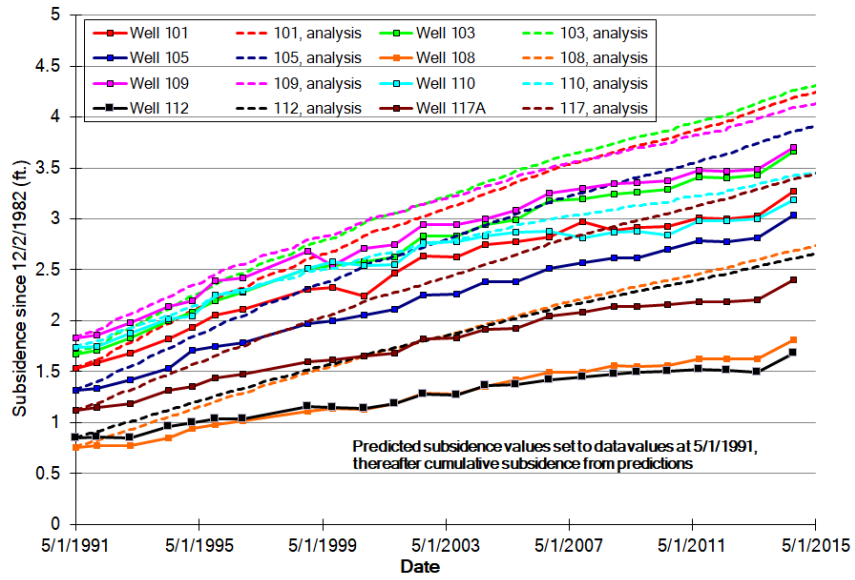


Figure 11. Comparison of West Hackberry predicted surface subsidence vs. measurements, original WH M-D properties plus low equivalent stress component (Mechanism 0).

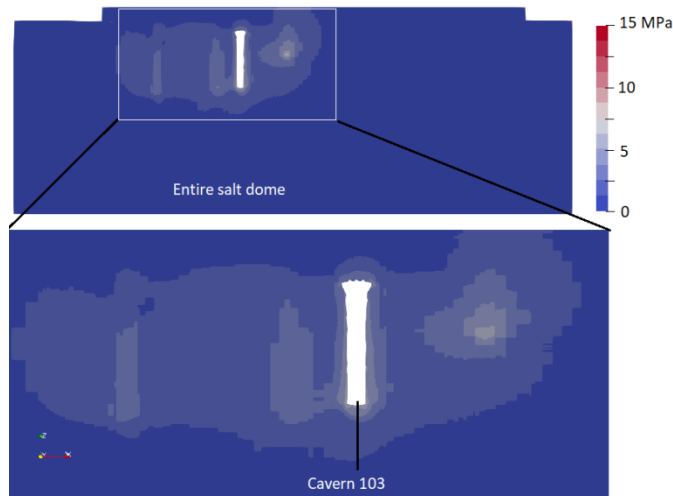


Figure 12. Contour plot of equivalent stresses (in MPa) across a west-east section near the center of the West Hackberry dome.

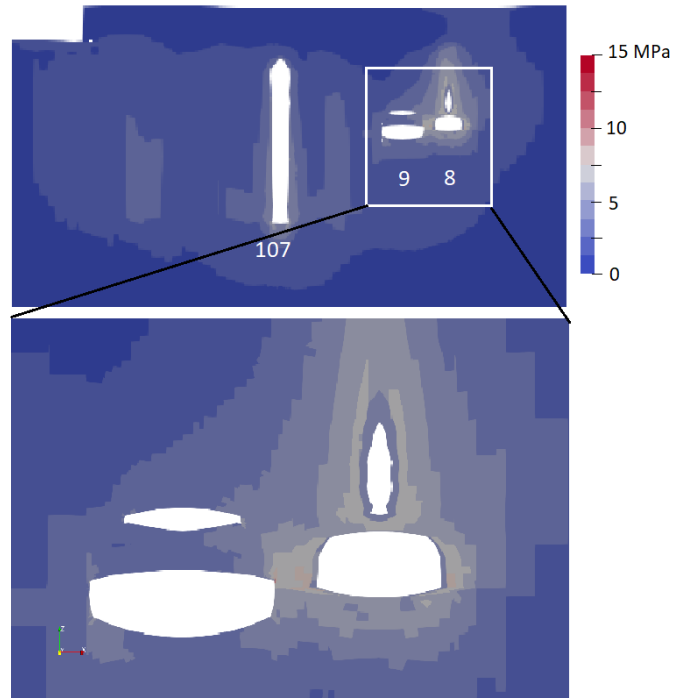


Figure 13. Contour plot of equivalent stresses (in MPa) across a west-east section in the vicinity of caverns 107, 9, and 8 of the West Hackberry dome.

To evaluate the range of effects that the Mechanism 0 creep coefficient A_0 may have on predictions of cavern volume closure and surface subsidence, an additional set of calculations was run. This set was like the set described for Figures 10-13, except it used a value for $A_0 = 26.75 \text{ sec}^{-11}$. Figure 14 shows the resulting predictions of cavern volume closure as compared to the measured values. When compared to Figure 10, the predicted steady-state creep rates are much closer to the measured values. Figure 15 shows the resulting predictions of surface subsidence as compared to the measured values. Once again, when compared to Figure 11, the predicted surface subsidence values are much closer to the measured values. Some of the predictions are slightly greater than the data, and some are slightly less. The results indicate that theoretically there is a value for A_0 that would create predictions that generally agree well quantitatively and qualitatively.

Both the measured and predicted results indicate a range of variability in the creep behavior of the salt that could still be estimated with cavern-specific multiplication factors applied to A_2 and A_0 . However, a better approach would be to calibrate the model against laboratory creep tests at low equivalent stresses on West Hackberry salt.

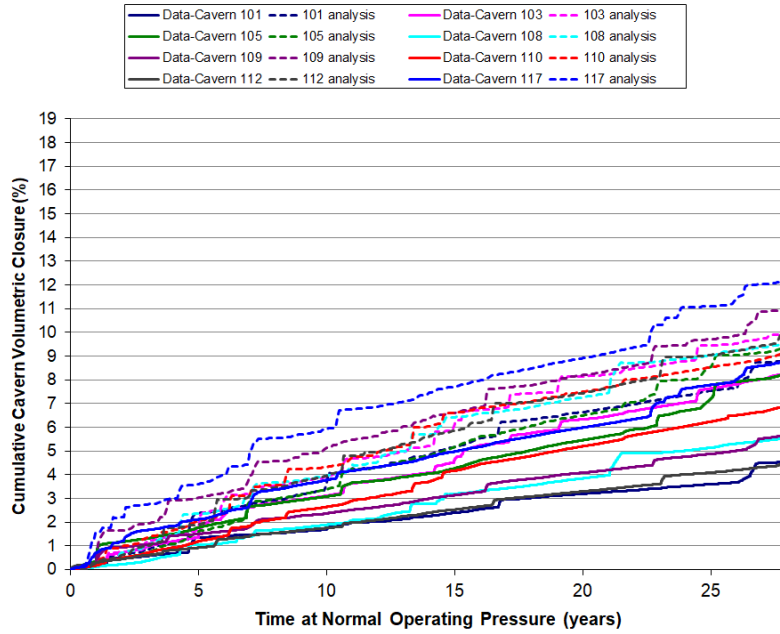


Figure 14. Comparison of West Hackberry predicted cavern closure vs. measurements, $A_0=26.75$.

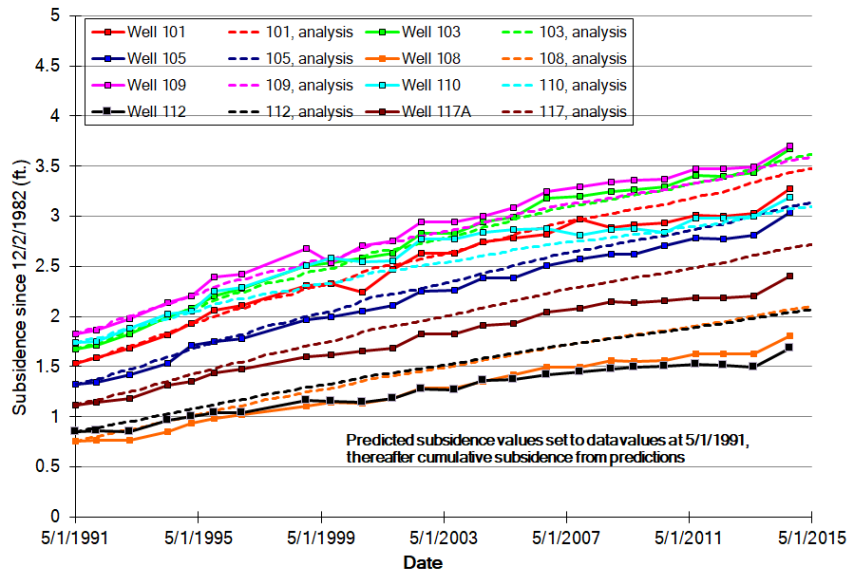


Figure 15. Comparison of West Hackberry predicted surface subsidence vs. measurements, $A_0=26.75$.

Predictions of subsidence and cavern closure

It is apparent from the previous figures that the addition of the creep mechanism at low equivalent stresses predicts displacement to be spread out over a larger volume of salt than does the original M-D model, and results in larger predictions for cavern volume closure and surface subsidence. For operational concerns, it is important to understand how this difference in predicted displacements affects predictions of cavern and wellbore casing integrity. Casing integrity is dependent upon the evolution of stresses around the caverns, as tensile or high shear stresses can result in tensile fracturing or in dilatant damage resulting in microfracturing and increase in permeability. These events can result in salt fall or loss of fluid into the salt formation. The potential for fracturing is particularly notable during cavern workovers, when the wellhead pressure is reduced to zero and the differential between cavern oil pressure and in situ pressure of the

surrounding salt is at its highest. Figure 16 compares the predicted maximum principal stress (negative numbers represent compression, positive are tension) using the two salt constitutive models for cavern WH-108 at the beginning of a workover, when the stress differential is at its highest. There is some slight difference in the distribution of stresses around the wall of the cavern, but the maximum value is essentially the same for both models (a difference of less than 3%, occurring near the top of the cavern). This makes sense, as the conservation of energy would suggest that the pressure in the salt would react to the pressure of the oil with equal force; the difference in creep models merely modifies the extent to which the salt deforms in response to the stress. Figure 17 shows a similar plot of the predicted square root of the second invariant J_2 of the deviatoric stress tensor, which is a measure of the shear stress. Higher levels of shear stresses can lead to dilatant deformation of the salt. The difference between models is more pronounced, as the predicted higher shear stresses are spread out over a larger volume for the M-D viscoplastic model. The maximum shear stress values predicted by the M-D viscoplastic model is approximately 30% higher than that predicted by the M-D model, with both occurring near the top of the cavern. This difference in predicted behavior may be important in evaluating the potential for salt falls in the cavern, which has the capacity to damage the hanging string and affect oil-brine interaction in the boreholes.

The effect of the addition of the low equivalent stress component is also apparent when looking at the predicted vertical (axial) strain in the salt along the wellbore casings. It is currently assumed that as the salt deforms alongside the casings, those strains are transmitted through the bond between the salt and cement, and cement with steel casings. One of the evaluation criteria used for predicting damage to steel casings is the onset of plastic deformation at a strain of 1.6 millistrains. Figure 18 shows the predicted vertical strain for a few wellbore locations, comparing results from the M-D and M-D Viscoplastic models. Strain is plotted as a function of the distance from the top of the cavern, going up to the salt /caprock interface. The strains are predicted to be highest near the top of the cavern. For caverns whose roofs are a more rounded shape, the maximum value tends to be right at the top of cavern. For caverns whose roofs are a flatter shape, the maximum strain is often around 100 feet above the top of the cavern, where the casing shoe and bottom of the wellbore casing are often located. Because the displacement of salt is spread out over a larger volume in the M-D Viscoplastic model, the strains near the top of the cavern are predicted to be smaller, as are the predicted lengths of casing that may exceed the 1.6 millistrain threshold. This difference in the predicted displacements and strains was found to be highly variable on the property values used for the low stress creep mechanism (Sobolik and Ross, 2021). Therefore, it is important to get reliable laboratory data on which to establish appropriate property values, so that the effect on predicted cavern and casing behavior can be better quantified.

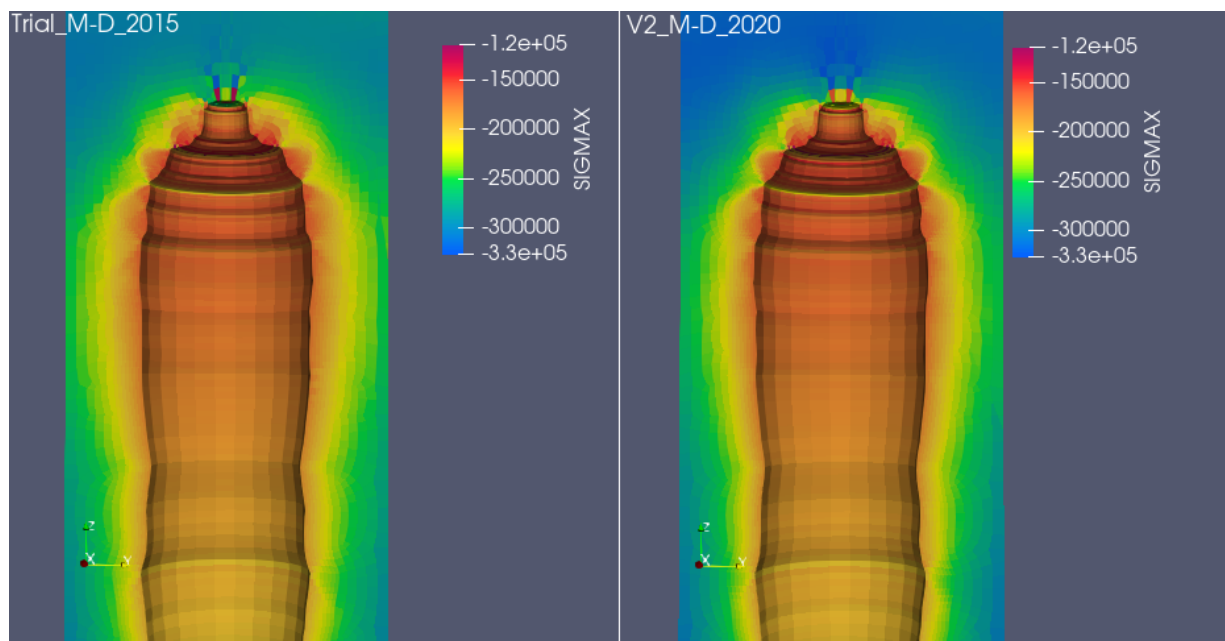


Figure 16. Predicted maximum principal stress (in pounds/square feet) around cavern WH-108 using the M-D model (left) and the M-D viscoplastic model (right).

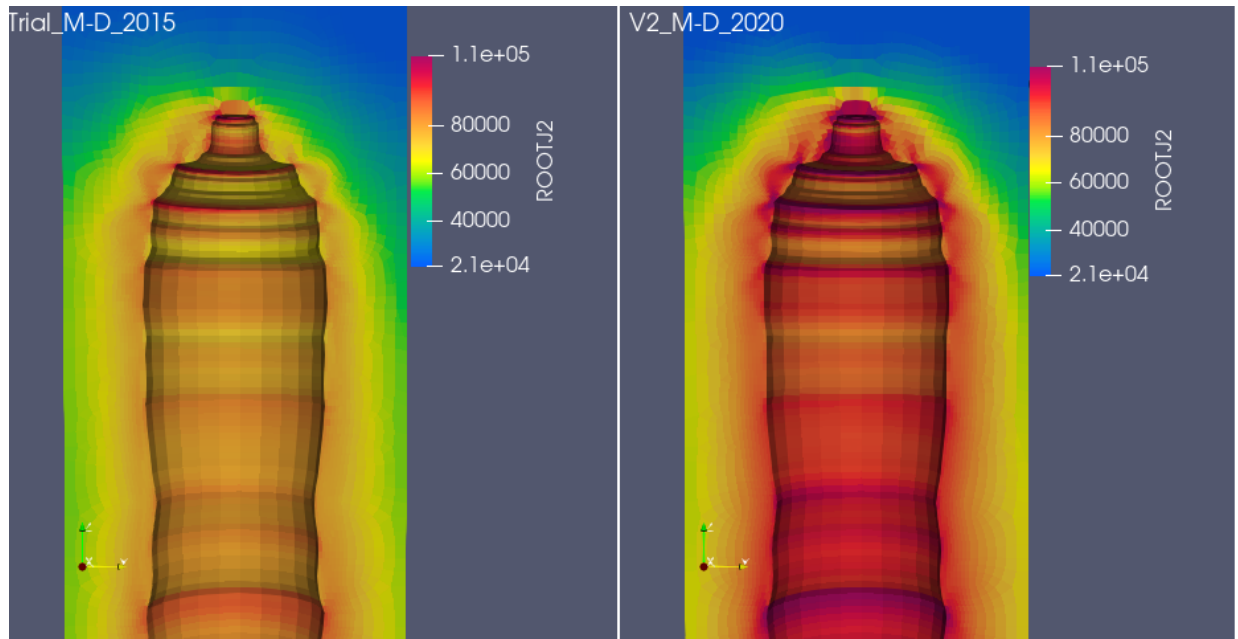


Figure 17. Predicted square root of second stress invariant (n pounds/square feet) around cavern WH-108 using the M-D model (left) and the M-D viscoplastic model (right).

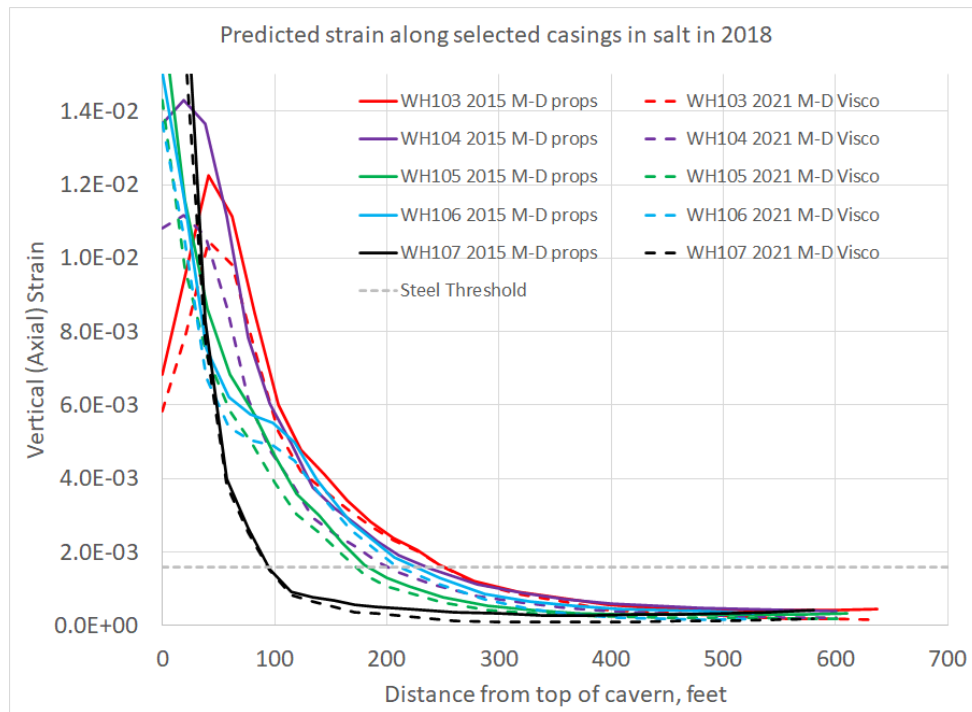


Figure 18. Predicted axial strain along wellbore casings for selected WH caverns using the M-D model and the M-D viscoplastic model.

Conclusions

A recent collaboration between US and German researchers characterized the creep behavior of salt at low equivalent stresses (<8 MPa). This research has resulted in an extension of the M-D model that includes a low stress creep mechanism. This extended M-D model, called the M-D Viscoplastic model, has

been used in Sandia's geomechanical models for the SPR. The results show that low stress creep is the dominant large-scale displacement mechanism at the dome scale. This discovery indicates the need for laboratory creep tests at low equivalent stresses on salt from storage cavern sites, such as the SPR. This knowledge will help to improve evaluation of storage cavern behavior in salt domes.

Acknowledgements

Sandia National Laboratories is a multimission laboratory managed and operated by National Technology and Engineering Solutions of Sandia, LLC., a wholly owned subsidiary of Honeywell International, Inc., for the U.S. Department of Energy's National Nuclear Security Administration under contract DE-NA0003525.

References

- Ballard, S. and B. L. Ehgartner, 2000. *CaveMan Version 3.0: A Software System for SPR Cavern Pressure Analysis*, SAND2000-1751, Sandia National Laboratories, Albuquerque, New Mexico.
- Bérest, P., Blum, P. A., Charpentier, J. P., Gharbi, H., and Valès, F. (2005). "Very slow creep tests on rock samples". In: *International Journal of Rock Mechanics and Mining Sciences* 42.4, pp. 569–576.
- Bérest, P., Béraud, J. F., Gharbi, H., Brouard, B., and DeVries, K. (2015). "A very slow creep test on an Avery Island salt sample". In: *Rock Mechanics and Rock Engineering* 48.6, pp. 2591–2602.
- Bérest, P., Gharbi, H., Brouard, B., Brückner, D., DeVries, K., Hévin, G., Hofer, G., Spiers, C., and Urai, J. (2019). "Very slow creep tests on salt samples". In: *Rock Mechanics and Rock Engineering* 52.9, pp. 2917–2934. doi: 10.1007/s00603-019-01778-9.
- Düsterloh, U., Herchen, K., Lux, K.-H., Salzer, K., Günther, R.-M., Minkley, W., Hampel, A., Argüello Jr, J. G., and Hansen, F. D. (2015). "Joint Project III on the comparison of constitutive models for the thermomechanical behavior of rock salt. III. Extensive laboratory test program with argillaceous salt from WIPP and comparison of test results". In: *Proc. 8th Conference on the Mechanical Behavior of Salt*. Ed. by L. Roberts, K. D. Mellegard, and F. D. Hansen, pp. 13–21.
- Hosford, W. (1972). "A generalized isotropic yield criterion". In: *Journal of Applied Mechanics*, 39.2, pp. 607–609.
- Munson, D.E. and P.R. Dawson, 1979. *Constitutive Model for the Low Temperature Creep of Salt (With Application to WIPP)*. SAND79-1853, Sandia National Laboratories, Albuquerque, New Mexico.
- Munson, D.E. and P.R. Dawson. 1982. *A Transient Creep Model for Salt during Stress Loading and Unloading*. SAND82-0962, Sandia National Laboratories, Albuquerque, New Mexico.
- Munson, D.E. and P.R. Dawson, 1984. Salt Constitutive Modeling using Mechanism Maps. *1st International Conference on the Mechanical Behavior of Salt, Trans Tech Publications, 717-737*, Clausthal, Germany.
- Munson, D.E., 1998. Analysis of Multistage and Other Creep Data for Domal Salts, SAND98-2276, Sandia National Laboratories, Albuquerque, New Mexico.
- Park, B.Y. (2020). Milestone 1.2a1: Geomechanical analysis using M-D viscoplastic material model – Big Hill (FY20), Letter to Diane Willard, DOE-SPR, July 31, 2020, Sandia National Laboratories, Albuquerque, NM USA. U.S. Strategic Petroleum Reserve.
- Peach, C., Spiers, C., and Trimby, P. (2001). "Effect of confining pressure on dilatation, recrystallization, and flow of rock salt at 150 C". In: *Journal of Geophysical Research: Solid Earth* 106.B7, pp. 13315–13328.
- Reedlunn, B. (2016). Reinvestigation into Closure Predictions of Room D at the Waste Isolation Pilot Plant. Tech. rep. SAND2016-9961. Albuquerque, NM, USA: Sandia National Laboratories.
- Reedlunn, B. (2018a). "Joint Project III on the Comparison of Constitutive Models for the Mechanical Behavior of Rock Salt: Reinvestigation into Isothermal Room Closure Predictions at the Waste Isolation Pilot Plant". In: *The Mechanical Behavior of Salt IX*. Ed. By S. Fahland, J. Hammer, F. D. H. Hansen, S. Heusermann, K.-H. Lux, and W. Minkley. BGR (Federal Institute for Geosciences and Natural Resources). isbn: 978-3-9814108-6-0.

- Reedlunn, B. (2018b). Enhancements to the Munson-Dawson Model for Rock Salt, SAND2018-12601, Sandia National Laboratories, Albuquerque, NM USA.
- Salzer, K., Günther, R.-M., Minkley, W., Naumann, D., Popp, T., Hampel, A., Lux, K.-H., Herchen, K., Düsterloh, U., Argüello Jr, J. G., and Hansen, F. D. (2015). "Joint Project III on the comparison of constitutive models for the thermomechanical behavior of rock salt. II. Extensive laboratory test program with clean salt from WIPP". In: Proc. 8th Conference on the Mechanical Behavior of Salt. Ed. by L. Roberts, K. D. Mellegard, and F. D. Hansen, pp. 3–12.
- Sierra/Solid Mechanics (2018). *Sierra/Solid Mechanics User's Guide. 4.50*. SAND2018-10673. Sandia National Laboratories. Albuquerque, NM, USA; Livermore, CA, USA.
- Sobolik, S. R. (2015). *Analysis of Cavern and Well Stability at the West Hackberry SPR Site Using a Full Dome Model*, SAND2015-7401, Sandia National Laboratories, Albuquerque, NM USA. U.S. Strategic Petroleum Reserve.
- Sobolik, S. R. (2018). *Analysis of Cavern and Well Stability at the Bryan Mound SPR Site Using the M-D Salt Creep Model*, SAND2018-9708, Sandia National Laboratories, Albuquerque, NM USA. U.S. Strategic Petroleum Reserve.
- Sobolik, S. R. (2019). *Milestone 1.2c1: BM model analysis enhancements – improved M-D model, caprock model, BM-3 model (FY19)*, Letter to Diane Willard, August 30, 2019, Sandia National Laboratories, Albuquerque, NM USA. U.S. Strategic Petroleum Reserve.
- Sobolik, S. R. (2020). *Milestone 1.2a2: Geomechanical analysis using MD viscoplastic material model – Bryan Mound (and West Hackberry)*, Letter to Diane Willard, August 17, 2020, Sandia National Laboratories, Albuquerque, NM USA. U.S. Strategic Petroleum Reserve.
- Sobolik, S.R. and T.S.A. Ross (2021). "Effect of the Addition of a Low Equivalent Stress Mechanism to the Analysis of Geomechanical Behavior of Oil Storage Caverns in Salt," ARMA 21-1127, 55th US Rock Mechanics / Geomechanics Symposium held online in Houston, Texas, USA, 20-23 June 2021.
- Ter Heege, J. d., De Bresser, J., and Spiers, C. (2005a). "Dynamic recrystallization of wet synthetic polycrystalline halite: dependence of grain size distribution on flow stress, temperature and strain". In: *Tectonophysics* 396.1-2, pp. 35–57. Distribution –37– October 8, 2020
- Ter Heege, J., De Bresser, J., and Spiers, C. (2005b). "Rheological behaviour of synthetic rocksalt: the interplay between water, dynamic recrystallization and deformation mechanisms". In: *Journal of Structural Geology* 27.6, pp. 948–963.
- Urai, J., Schléder, Z., Spiers, C., and Kukla, P. (2008). "Flow and transport properties of salt rocks". In: *Dynamics of complex intracontinental basins: The central European basin system*, pp. 277–290.